PERFORMANCE COMPARISON OF TCSC AND SPLIT TCSC UNDER ATC ENHANCEMENT THROUGH PLANT ROOT FORAGING ALGORITHM

L.JEBARAJ*
M.I.E.T Engineering College, Trichy, Tamil Nadu, India,

I.SOUBACHE
Rajiv Gandhi College of Engineering and Technology, Puducherry, India,

C.CHRISTOBER ASIR RAJAN
Pondicherry Engineering College, Puducherry, India,
*Corresponding Author E-mail: jebarajjebin@gmail.com

Abstract: *Available Transfer Capability (ATC) improvement and determination are imperative issues in deregulated operation of power systems. This paper investigates the use of Flexible AC Transmission System (FACTS) devices, like Thyristor Controlled Series Capacitor (TCSC) and split TCSC to make best use of power transfer transactions during normal state of affairs. ATC is computed using Continuation Power Flow (CPF) method and AC power transfer distribution factors (ACPTDF) determination. A new plant Root Foraging Algorithm (PRFA) is used as an optimization tool to determine the location and controlling strictures of TCSC and split TCSC. The suggested methodology is tested on IEEE 30-bus and IEEE 57-bus test system.*

Key words: *FACTS Devices, ATC, TCSC, Continuation Power Flow, Jacobian Matrix.*

1. Introduction.

Restructuring of electric industry is aspiring to egg on cut-throat markets for dealing of electric power. The major effect of the non-prejudiced open-admittance prerequisite is the considerable amplify in power transfers under new-fangled background. The un-exploited transfer abilities of a transmission network for the transport of power intended for additional commercial activity, in addition to by now dedicated usage is named as the Available Transfer Capability (ATC) of a transmission network. ATC in sufficient level helps to make sure every economically based deal to make easy for liquidity power market. Sometimes the existing transmission amenities are may be rigorously used owing to the state of affairs [1].

The terminal voltages are attuned by several ATC approaches and enhance the postponement generation. The determination of ATC [2] through continuation power flow (CPF) is to find the utmost scalar parameter values which varies in a group of buses under nodal injections [3]. Utmost utilization of subsisting transmission benefits will be additional lucrative for clients and possessors of transmission system will be given better services with abridged costs [4]. The calculation of ATC under DC load flow based techniques incorporating DC power transfer distribution factors (DCPTDF) are reported in [5-6]. A number of precise approaches of calculating ATC through AC load flow methods incorporating the consequence of voltage limits, reactive power flows [7], AC load flow incorporating sensitivity factors [8-11] and integrating first order sensitivity of the transfer capability [12] are also been reported . The bilateral and concurrent transaction environment based ATC computation is proposed by Li and Liu [13]. The calculation of ATC with ACPTDF for multi-transactions and the comparison between AC and DC PTDF technique are presented in [14]. FACTS devices play an imperative role to enhance the ATC in effectual manner and hopeful option to traditional methods. Such devices are superior in control amenities for both static and dynamic control of stability [15-18]. In this paper the ATC computation is obtained from CPF and ACPTDF incorporating with variable reactance model of TCSC [19] and Split TCSC [20] devices through Plant Root Foraging Algorithm [21]. Simulation results have been carried out with IEEE 30 and 57 bus test cases.

2. Modeling of Single TCSC.

2.1. Basic Firing Angle Model

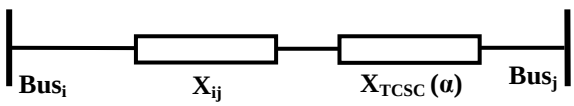

Fig 1: Transmission line with single TCSC

TCSC is a series type FACTS device which controls the line reactance when connected in series with the transmission line between Bus_i and Bus_j as exposed in figure 1. It can operate either in inductive mode (+) or in capacitive mode. Therefore the equivalent reactance of the transmission line becomes

$$X_{Total} = X_{ij} \pm X_{TCSC}(\alpha) \quad (1)$$

The term α denotes the firing angle of TCSC varies from $90°$ to$180°$. Effective TCSC reactance

X_{TCSC} with regard to firing angle (α) can be specified as:

$$X_{TCSC}(\alpha) = -X_C + C_1(2(\pi-\alpha) + \sin(2(\pi-\alpha))) - C_2(cos^2(\pi - \alpha)(\omega \tan(\omega(\pi-\alpha) - \tan(\pi-\alpha)) \quad (2)$$

where

$$C_1 = \frac{X_c + X_L}{\pi} \quad (3)$$

$$C_2 = 4\frac{1}{X_L \pi}\left(\frac{X_C X_L}{X_C - X_L}\right)^2 \quad (4)$$

$$\omega = \sqrt{\frac{X_C}{X_L}} \quad (5)$$

X_L = Inductive reactance
X_C = Capacitive reactance

2.2. Proposed Variable Reactance Model

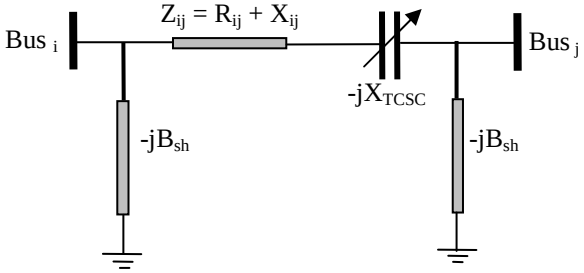

Fig. 2: Variable reactance model of TCSC

TCSC consists of a group of capacitors in series which is shunted by thyristor controlled reactor. The power flow control is obtained by TCSC with reduce or add to the overall line effectual series transmission impedance, by adding together a capacitive or inductive reactance in that order. The variable reactance type of TCSC is proposed in this paper. The model of variable reactance type of TCSC is depicted in figure 2. The equivalent reactance of line X_{ij} is defined as:

$$X_{ij} = -0.8X_{line} \leq X_{TCSC} \leq 0.2X_{line} \quad (6)$$

where, X_{line} is the transmission line reactance, and X_{TCSC} is the TCSC reactance. The level of the applied compensation of the TCSC typically varies flanked by 20% inductive and 80% capacitive.

3. Modeling of Split TCSC.

3.1 Basic Firing Angle Model

The split TCSC is a series grouping of two single TCSC which is connected in the transmission line between the bus_i and bus_j as shown figure 3. The reactance value is splitted in terms of ratio of degree of series compensation ($c = c_1 + c_2$). The degree of series compensations c_1 and c_2 are properly chosen to get extensive and fine reactance compensation in the network. Both the TCSC's are well tuned and fine tuning of line reactance are attained. Thus, the resultant line reactance is given by

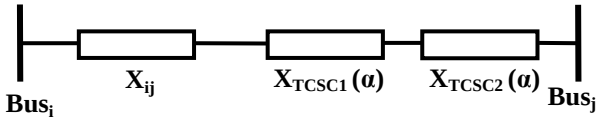

Fig. 3 Transmission line with split TCSC

$$X_{Total} = X_{ij} \pm X_{TCSC1}(\alpha_1) \pm X_{TCSC2}(\alpha_2) \quad (7)$$

where α_1 and α_2 are firing angles of split TCSC, each can be tuned independently between 90^0 to 180^0. Considering 'n' number of possible firing steps between 90^0 and 180^0, *[n x n]* firing points are possible for split TCSC. Apart from tuning, each TCSC can operate alone in cut off mode. So that reactance values [(n + 1) x (n + 1)] are probable for compensation. The net reactance is also given by

$$X_{Total} = X_{ij} \pm X_{se}[(\alpha_{1n+1}) \pm X_{TCSC2}(\alpha_{2n+2})] \quad (8)$$

$$X_{se}[(\alpha_{1n+1}) \text{ x } (\alpha_{2n+2})] = \begin{bmatrix} X_{se}(1,1) & \cdots & X_{se}(1,n) & X_{TCSC2}(1) \\ \vdots & \ddots & \vdots & \vdots \\ X_{se}(1,1) & \ldots & X_{se}(n,n) & X_{TCSC2}(n) \\ X_{TCSC1}(1) & \ldots & X_{TCSC1}(n) & Both\ in\ cutoff \end{bmatrix} \quad (9)$$

where $X_{se}(S_1,S_2) = [X_{TCSC1}(S_1) \pm X_{TCSC1}(S_2)]$, both S_1 and S_2 varies from 1 to n. Hence, fine tuning of reactance is possible by splitting the TCSC device.

3.2 Proposed Variable Reactance Model

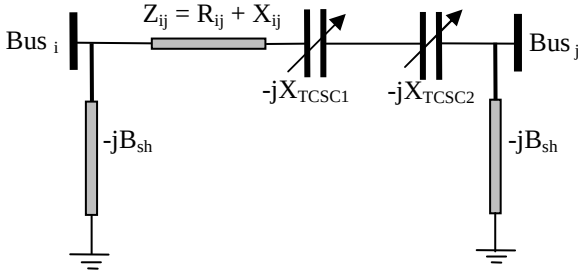

Fig. 4: Variable reactance model of Split TCSC

The proposed variable reactance type model of Split TCSC is depicted in figure 4. The equivalent reactance of line X_{ij} is defined as:

$$X_{ij} = X_{ij1} \pm X_{ij2} \quad (10)$$

where

$$X_{ij1} = -0.8X_{line} \leq X_{TCSC1} \leq -0.5X_{line} \quad (11)$$

$$X_{ij2} = -0.5X_{line} \leq X_{TCSC2} \leq 0.2X_{line} \quad (12)$$

where, X_{line} is the transmission line reactance, X_{TCSC1} and X_{TCSC2} are the Split TCSC reactance. The level of the applied compensation of the Split TCSC typically varies between 80% capacitive to 50% capacitive for $TCSC_1$ and between 50% capacitive to 20% inductive for $TCSC_2$.

4. Overview of Plant Root Foraging Algorithm

McNickle et al [22] proposed a new root foraging behaviour in which the root system tropism behaviours like hydrotropism and gravitropism. The gravitropism induces plant roots cultivate along a precise vector relative to gravity whereas hydrotropism is the root morphological rejoinder is guided by a gradient in nutrition concentration. Auxin plays an imperative role in conducting these tropism behaviours, influencing concurrently the spatial formation of the roots system. Some of the important criteria are given here so as to idealize above plant root foraging behaviours.

Auxin Regulation: The adaptive growth and the information swap among root leans are conducted by auxin. Auxin concentration as well regulates the roots spatial structure which is but dynamically reallocated after new roots germinate and grow.

Root Growth Behaviour: Roots are being capable of grow longer with a convinced angle. The evolution for multiplying the number of roots named as branching wherein new roots instigate from it and the parent root tip by a convinced elongate-unit in new route.

Classification of root System: The entire plant root system can be classified in to three types like major roots, the lateral-roots, and the dead-roots which can be sorted by the auxin distribution. Every root tilt of major roots can put into practice both branching and re-growing wherein the branching number is resolved by auxin attention. The root tips of lateral roots are able to merely execute re-growing operation.

Root Tropisms: Root pretentious by a variety of tropisms develops in the direction of the most nutrient wealthy location. The rising direction of the root tips in the direction of the best individual location made by Hydrotropism. Intervening time gravitropism inflicts that roots grow in the direction of gravitational pull downward, which means that the growing angle of every root tilt is limited to a sure range.

4.1 Auxin Information

The growth points and branching number of roots are keeping pace by auxin information. Let us presume that the sum of auxin concentration C_i is considered as 1 in the mathematical model of root systems. So as to compute the C_i value of every root given as,

$$f_i = \frac{fit_i - f_{worst}}{f_{best} - f_{worst}} \tag{13}$$

$$N_i = \frac{Nutition_i - Nutition_{worst}}{Nutition_{best} - Nutition_{worst}} \tag{14}$$

$$C_i = \frac{f_i}{\sum_{j=1}^{N} f_i} * \sigma + \frac{N_i}{\sum_{j=1}^{N} N_i}(1 - \sigma),\ \ \sigma \subset (0,1) \tag{15}$$

where i is the growing point position, σ is a uniform random quantity, N is the total number of the points, fit $(\cdot)$ is the fitness value of the point, and f_{worst} and f_{best} are the maximum and minimum of the current points, respectively. $Nutrition_i$ is the current nutrient concentration of individual i. Besides the objective function value, the auxin concentration is as well determined by the gradient of function fitness. The idea of nutrient concentration to replicate the moisture gradient of soil environment is expressed as

$$Nutition_i(t+1) = \begin{cases} Nutition_i\,(t) + 1, & if \quad f_i(t+1) < f_i(t), \\ Nutition_i\,(t) - 1, if & \quad f_i(t+1) > f_i(t). \end{cases} \tag{16}$$

Nutrient concentration reveals that even if the amount of moisture is not best, the higher moisture gradient of the soil is also conducive to the root cell division to absorb water and nutrition.

4.2 Re-growing Operator

Derived from the mathematic expression the re-growing operator can be portrayed as follows.

Step 1: The number of the roots chosen as main roots is defined by

$$S = N \times Cr, \tag{17}$$

where S is the size of main roots group, N is the total number of the roots, and Cr is the selection probability.

Step 2: Choose current main roots to search in the direction of the optimal position of individuals under hydrotropism:

$$U_i(t+1) = U_i(t) + rand_1\big(X_{best} - U_i(t)\big) \tag{18}$$

Step 3: New growing points of rest main roots can be devised under gravitropism as

$$U_i(t+1) = U_i(t) + rand_2\big(Grow_{max} - D_i(\varphi)\big) \tag{19}$$

Step 4: The growth angle depiction of the main root i is defined by

$$\varphi_i(t+1) = \varphi_i(t) + rand_3 \times \alpha_{max} + rand_4 \times \pi, \alpha_{max} < \pi, \tag{20}$$

where $rand_1, rand_3$ and $rand_4$ are random coefficients varying from 0 to 1, $rand_2$ is a normally distributed random number with mean 0 and standard deviation 1, $Grow_{max}$ is the entire growing angle space limited to π $D_i(\varphi_i)$ is the growth direction.

4.3 Branching operator

The branching operator is the local search scheme to use around the optimal area wherein the new roots under major roots branch using a little elongate-length unit. The process can be portrayed as follows.

Step 1*:* The nutrient concentration (Nutrition_i) of mainroot i is evaluated with the doorsill value Branch$G$ (satisfied 0 < Branch$G$ < 1) to conclude whether it executes branching operator by

$$branching,\ if\ Nutition_i\ >\ BranchG,\\ nobranching,\ otherwise. \quad (21)$$

Step 2: Resolve the branching number $w_i$according to the auxin concentration distribution.

$$w_i = \begin{cases} S_{min}C_i\ \times r\ \times (S_{max}-\ S_{min})+\ S_{min}, \\ \quad if\ Nutition_i > BranchG, \\ \quad 0, \\ \quad else, \end{cases} \quad (22)$$

where S_{max} and S_{min} are the maximum and minimum of the new growing points, respectively, and r is random distribution coefficient. C_i is auxin concentration of main root i.

Step 3: Fitness calculation for new branching points and the searching angle space is divided into $S_{\max}$ subzones. The angle of new growing point is arbitrarily falling in one of $S_{\max}$ angle subzones concerning the growth direction of the preliminary major root as zero degree. The new rising point equation is articulated as

$$U_i(t+1) =\ U_i(t) +\ rand_5\ \times D_i(\varphi), \quad (23)$$

where $U_i(t+1)$ is the new growing point from $U_i(t), rand_5$ is the elongate-length unit, which is an arbitrary altering from 0 to 1, φ_i is the growth angle $(\varphi_{i1}, \varphi_{i2}, \dots, \varphi_{i(D-1)})$, and the growth direction $D_i(\varphi_i) = (d_{i1}, d_{i2}, \dots, d_{iD})$ which can be designed from φ_i by means of a Polar to Cartesian coordinates transformation like as

$$d_{i1} = \prod_{k=1}^{D-1}\cos(\varphi_{ik}),\quad d_{ij} = \sin(\varphi_{ij})\prod_{k=1}^{D-1}\cos(\varphi_{ik}), d_i^D = \sin(\varphi_i^{D-1}). \quad (24)$$

The growth angle $\varphi_i$is designed as

$$\varphi(t+) - \varphi(t) + rand_6\alpha_{init} + \frac{K\times\beta_{max}}{S_{max}}, \quad (25)$$

where $rand_6$ is a random coefficient varying from 0 to 1, α_{init} is original growth angle value of the initial major root as zero degree, K is arbitrarily parameter selecting the subzone, S_{max} is subzones number, and β_{max} is the utmost growing turning angle. In view of gravitropism the growing angle space $\beta_{max}$is limited to π to make major roots tend to grow downwards.

4.4 Lateral-Roots growth operation

The lateral-roots group with lower auxin concentration stays in the preliminary growth phase, its elongation step is comparatively little and the influence of the hydrotropism can be mistreated. The lateral-roots with the lesser elongation step are using a local optimal area, which closed to its original point. These actions can be defined as

$$U_i(t+1) =\ U_i(t) +\ rand_3 \times Grow_{max} \times D_i(\varphi)\ , \quad (26)$$

$$\varphi_i(t+1) = \varphi_i(t) +\ rand_4\alpha_{max}, \quad (27)$$

4.5 Dead-Roots elimination.

Assumed that if the dimension of current population N_i will augment by one if a root tilt splits and decrease by one if a root dies resolute by auxin allocation and it will differ in the searching procedure. The branching principle and dead roots eliminating decisive factor are articulated as

$$N_i = N_i + w_i\ \ if\ F_i > BranchG, N_i = N_i - 1,\quad if\ F_i > N_{mority} \quad (28)$$

Where w_i is the branching number, $BranchG$ is the branching threshold value and N_{mority} is the death threshold value parameter.

5. Problem Formulation

5.1 Algorithm for ATC calculation using CPF

Step 1: Read the system line data and bus data:

(i) Line resistance, line reactance, half line charging admittance, maximum line flows, Bus no., Bus type, $P_{generated}$, $Q_{generated}$, and P_{Load}, Q_{Load}, P_{min}, P_{max} and shunt capacitance data.

(ii) Calculate $P_{sheduled}$(i), $Q_{sheduled}$(i), for i = 1 to n

where $P_{sheduled}$(i) = $P_{generated}$ (i) − P_{Load} (i)

$Q_{sheduled}$ (i) = $Q_{generated}$ (i) − Q_{Load} (i)

(iii) Form Y-bus using sparsity technique

Step 2: Iter = 1 iteration count

(i) Set $|\Delta P_{max}| = 0$ and $|\Delta Q_{max}| = 0$

(ii) Calculate P and Q

$$P_{calculated}(i) = \sum_{p=1}^{n}|V_i|\,|V_q|\,|Y_{iq}|\cos(\delta_{iq}-\theta_{iq})$$

$$Q_{calculated}(i) = \sum_{q=1}^{n}|V_i|\,|V_q|\,|Y_{iq}|\,sin(\delta_{iq}-\theta_{iq})$$

(iii) Calculate P(i) and Q(i)

P(i) = $P_{sheduled}$ (i) − $P_{calculated}$ (i)

Q (i) = $Q_{sheduled}$ (i) - $Q_{calculated}$ (i) for i = 1 to n

Set P_{slack}= 0.0, Q_{slack}= 0.0

(iv) Calculate $|\Delta P_{max}|$ and $|\Delta Q_{max}|$ form [ΔP] and [ΔQ] vectors

Is $|\Delta P^{max}| \leq \in$ and $|\Delta Q^{max}| \leq \in$; If yes go to step 7, problem converged case.

Step 3: Form Jacobian elements

(i) Initialize A[i][j] = 0 for i = 1 to 2n + 2 and j = 1 to 2n + 2

(ii) Form diagonal elements for i = 1 to (2n + 2)

$$H_{pp} = \frac{\partial P_P}{\partial \delta_P} = -Q_P - B_{PP}\,|Vp|^2$$

$$N_{pp} = \frac{\partial P_P\,|Vp|}{\partial V_P} = P_P + G_{PP}\,|Vp|^2$$

$$M_{pp} = \frac{\partial Q_P}{\partial \delta_P} = P_P - G_{PP}\,|Vp|^2$$

$$L_{pp} = \frac{\partial Q_P\,|Vp|}{\partial V_P} = Q_P - B_{PP}\,|Vp|^2$$

(iii) Formation of off diagonal elements

$$H_{pq} = \frac{\partial P_P}{\partial \delta_P} = |V_P||V_q|(G_{Pq}\sin\delta_{Pq} - B_{Pq}\,cos\,\delta_{Pq})$$

$$N_{pq} = \frac{\partial P_P\,|Vq|}{\partial V_q} = |V_P||V_q|(G_{Pq}\cos\delta_{Pq} + B_{Pq}\,sin\,\delta_{Pq})$$

$$M_{pq} = \frac{\partial Q_P}{\partial \delta_q} = -N_{pq}$$

$$L_{pq} = \frac{\partial Q_P\,|Vq|}{\partial V_q} = H_{pq}$$

(iv) Modification of Jacobian elements for slack bus and generator buses

For slack bus

$H_{pp} = 10^{20}$

$L_{pp} = 10^{20}$

For PV buses $L_{pp} = 10^{20}$

(v) Jacobian correction mismatch vector

B[i] = ΔP[i], B[i + n] = ΔQ[i] for i = 1 to n

Step 4: Use Gauss-elimination method for solving [A][ΔX] = [B]

Update the phase angle and voltage magnitudes

for i = 1 to n

δi = δi + ΔXi

$V_i = V_i + \{\Delta X_{i+n}\}V_i$

Step 5: Completion of first iteration

Advance iteration count iter = iter + 1

If (iter > $iter_{max}$) go to step 2 (i)

Else go to step 6

Step 6: NR not converged in ''$iter_{max}$'' iterations

Step 7: NR converged in 'iter' iterations

Calculate Line flows, Bus powers, slack bus power and Print the converged voltages, line flows and powers

Step 8: Read the sending bus (seller bus) m and the receiving bus (buyer bus) n

Step 9: Assume some positive real power injection change Δtp (=0.1)

i.e. λ-factor at seller bus-m and negative injection Δtp (=0.1), i.e. λ-factor at the buyer bus-n and form mismatch vector

Step10: Repeat the load flow

(i.e., from steps 2 to 7) and from the new line flows check whether any of the line is overloaded. If yes stop the repeated power flow else go to step 9

Step11: The maximum possible increment achieved above base-case load at the sink bus is the ATC

5.2 Formulation of ACPTDF

The changes in power injection on power system constituents are concluded by ACPTDF. These values provide a linearised approximation of the mode of transmission line flow and boundary of change in response to between the buyer and seller transactions. Considering a seller bus *r* and buyer bus *s* having a bilateral transaction T_b between them with a line *l* carries the part of the transacted power and is connected between buses *i* and *j*. The transaction flanked by the buyer and seller for real power transaction is ΔT_b MW with the change in a transmission line quantity q_1 is Δ_{q1}; the PTDF can be defined as

$$ACPTDF_{ij,rs} = \frac{\Delta q_l}{\Delta T_b} \qquad (28)$$

The transmission quantity q_l can be either real power flow from bus *i* to bus *j* (P_{ij}) or real power flow from bus *j* to bus *i* (P_{ji}). The above issues have been projected to calculate at a base case load flow using the sensitivity properties of NRLF Jacobian. Consider full Jacobian in polar coordinates [J_T], which is defined to comprise all the buses except slack, we get the following:

$$\begin{bmatrix}\Delta\delta\\ \Delta V\end{bmatrix} = \begin{bmatrix}\frac{\partial P}{\partial \delta} & \frac{\partial P}{\partial V}\\ \frac{\partial Q}{\partial \delta} & \frac{\partial Q}{\partial V}\end{bmatrix}^{-1}\begin{bmatrix}\Delta P\\ \Delta Q\end{bmatrix} = [J_T]^{-1}\begin{bmatrix}\Delta P\\ \Delta Q\end{bmatrix} \qquad (29)$$

In a base case load flow, if only one of the k^{th} bilateral transactions is changed by ΔT_b MW, only the following two entries in the mismatch vector on right hand side of will be non zero.

$$\Delta P_i = \Delta T_b \qquad \Delta P_j = \Delta T_b \qquad (30)$$

The new voltage profile can be calculated by the change in voltage angle and magnitude at all buses computed from equations (29) and (30).

5.3 ATC Determination incorporating FACTS devices

With the determination of PTDFs with FACTS devices, the ATC can be determined for any number of transactions. FACTS for any transaction between seller bus r to buyer bus s can be obtained as:

$$P_{ij-rs,FACTS}^{max} = \begin{cases} \dfrac{Limit\ t_{ij}^{max} - P_{ij}}{PTDF_{rs,FACTS}^{ij}}; & PTDF_{rs,FACTS}^{ij} > 0 \\ \infty(infinite); & PTDF_{rs,FACTS}^{ij} = 0 \\ -\dfrac{Limit\ t_{ij}^{max} - P_{ij}}{PTDF_{rs,FACTS}^{ij}}; & PTDF_{rs,FACTS}^{ij} < 0 \end{cases} \quad (31)$$

where P_{ij} is the real power flow through any line i to j.

5.4 Determination of PTDF incorporating FACTS devices

Intended for a change in the transmission line quantity ΔP_{ij} for a transaction P_{rs} among the seller and buyer buses with FACTS devices, the AC power transfer distribution factors can be defined as,

$$PTDF_{rs,FACTS}^{ij} = \frac{\Delta P_{ij}^{FACTS}}{P_{rs}} \quad (32)$$

Intended for PTDF calculations with FACTS devices, the power flow sensitivity and N–R load flow Jacobian can be calculated. The power flow equations without FACTS devices in polar form can be represented as:

$$P_i = \sum_{j=1}^{n} |V_i||V_j||V_{ij}|cos\left(\theta_{ij} - \delta_i + \delta_j\right) \quad (33)$$

$$Q_i = \sum_{j=1}^{n} |V_i||V_j||V_{ij}|sin\left(\theta_{ij} - \delta_i + \delta_j\right) \quad (34)$$

Using Taylor series expansion, the change in power flows at any bus i can be formulated in terms of Jacobian as:

$$\begin{bmatrix}\Delta P \\ \Delta Q\end{bmatrix} = \begin{bmatrix}J_{1,FACTS} J_{2,FACTS} \\ J_{3,FACTS} J_{4,FACTS}\end{bmatrix} \begin{bmatrix}\Delta\delta^{FACTS} \\ \Delta|V|^{FACTS}\end{bmatrix} \quad (35)$$

where

$$[J_1]_{FACTS} = \frac{\partial P}{\partial \delta}; [J_2]_{FACTS} \frac{\partial P}{\partial |V|};$$

$$[J_3]_{FACTS} \frac{\partial Q}{\partial \delta}; [J_4]_{FACTS} \frac{\partial Q}{\partial |V|} \quad (36)$$

The change in the angle and voltage magnitude can be determined as:

$$\begin{bmatrix}\Delta\delta^{FACTS} \\ \Delta|V|^{FACTS}\end{bmatrix} = \begin{bmatrix}J_{1,FACTS} J_{2,FACTS} \\ J_{3,FACTS} J_{4,FACTS}\end{bmatrix}^{-1} \begin{bmatrix}\Delta P \\ \Delta Q\end{bmatrix} \quad (37)$$

The voltage magnitudes and angles can thus be obtained with FACTS devices through N–R load flow analysis. For calculation of PTDFs, the power flow sensitivity can be determined using the power flow equations with FACTS devices. Using Taylor's series approximation and ignoring higher order terms, change in real power flow can be written as:

$$\Delta P_{ij}^{FACTS} = \frac{\partial P_{ij}^{FACTS}}{\partial \delta_i^{FACTS}} \Delta\delta_i^{FACTS} + \frac{\partial P_{ij}^{FACTS}}{\partial \delta_i^{FACTS}} \Delta\delta_j^{FACTS} + \frac{\partial P_{ij}^{FACTS}}{\partial V_i^{FACTS}} \Delta V_i^{FACTS} + \frac{\partial P_{ij}^{FACTS}}{\partial V_i^{FACTS}} \Delta V_j^{FACTS} \quad (38)$$

The sensitivity coefficients in (37) can be obtained taking the partial derivatives of real power flows. The sensitivity of power flow equation can be written in the compact matrix form as:

$$\Delta P_{ij}^{FACTS} = \left[\frac{\partial P_{ij}^{FACTS}}{\partial \delta_2^{FACTS}}, \cdots, \frac{\partial P_{ij}^{FACTS}}{\partial \delta_n^{FACTS}} \quad \frac{\partial P_{ij}^{FACTS}}{\partial V_2^{FACTS}}, \cdots, \frac{\partial P_{ij}^{FACTS}}{\partial V_n^{FACTS}}\right] \begin{bmatrix}\Delta\delta_2^{FACTS} \\ \vdots \\ \Delta\delta_n^{FACTS} \\ \Delta[V_2^{FACTS}] \\ \vdots \\ \Delta[V_n^{FACTS}]\end{bmatrix} \quad (39)$$

For a bilateral transaction amount T_b between seller bus m and buyer bus n, and substituting in power injection column vector at its respective position. The change in power flows can be obtained as,

$$\Delta P_{ij}^{FACTS} = \left[\frac{\partial P_{ij}^{FACTS}}{\partial \delta_2^{FACTS}}, \cdots, \frac{\partial P_{ij}^{FACTS}}{\partial \delta_n^{FACTS}} \quad \frac{\partial P_{ij}^{FACTS}}{\partial V_2^{FACTS}}, \cdots, \frac{\partial P_{ij}^{FACTS}}{\partial V_n^{FACTS}}\right] \begin{bmatrix}J_{1,FACTS} & J_{2,FACTS} \\ J_{3,FACTS} & J_{4,FACTS}\end{bmatrix}^{-1} \begin{bmatrix}0 \\ \vdots \\ +T_b \\ 0 \\ \vdots \\ -T_b \\ 0\end{bmatrix} = PTDF_{mn,FACTS}^{ij} \times T_b \quad (40)$$

Therefore, the PTDFs with FACTS devices for

bilateral transaction can be represented as:

$$PTDF_{rs,FACTS}^{ij} = \left[\frac{\partial P_{ij}^{FACTS}}{\partial \delta_2^{FACTS}}, \cdots, \frac{\partial P_{ij}^{FACTS}}{\partial \delta_n^{FACTS}} \quad \frac{\partial P_{ij}^{FACTS}}{\partial V_2^{FACTS}}, \cdots, \frac{\partial P_{ij}^{FACTS}}{\partial V_n^{FACTS}}\right]$$

$$\begin{bmatrix} J_{1,FACTS} & J_{2,FACTS} \\ J_{3,FACTS} & J_{4,FACTS} \end{bmatrix}^{-1} \begin{bmatrix} 0 \\ \vdots \\ +1 \\ 0 \\ \vdots \\ -1 \\ 0 \end{bmatrix} \quad (41)$$

5.5 Determination of PTDF for Bilateral/Multi-lateral Transactions incorporating FACTS devices

For the duration of trading of power in a hybrid markets When ATC is determined for more than one transactions occurring concurrently in a system, ATC in such a case is called as simultaneous or multi-transaction ATC. The procedure for simultaneous ATC is similar as discussed for single transactions case with a change in the power injection matrix. In the simultaneous ATC case, the power injection matrix can be modified based on the transactions occurring between many sellers r, p and buyers s, q respectively. The change in power injection vector with multi-lateral transactions can be represented as:

$$\Delta P = \begin{bmatrix} 0 \\ (r) + P_t \\ \vdots \\ (p) - P_t \\ 0 \\ (s) + P_t \\ \vdots \\ (q) - P_t \\ 0 \end{bmatrix} \quad (42)$$

5.6 Optimal control parameters of PRFA

Table 1
Parameters of ARFO algorithm for optimization

Optimization setting	Values
The number of initial roots	1
The number of initial population	20
The maximum number of population	50
Number of Branches	20
Selection Probability	0.5
Minimum new growing point (S_{min})	0.0
Maximum new growing point (S_{max})	1.0
Minimum growth angle (α_{min})	0.0
Maximum growth angle (α_{max})	1.0

The different control parameter settings of plant root foraging algorithm in given in Table.1 regarding continuation power flow based available transfer capability incorporating TCSC and split TCSC.

6. Results and Discussion

The projected work is coded in MATLAB 7.6 platform using 2.8 GHz Intel Core 2 Duo processor based PC. The effectiveness of the proposed method is tested with IEEE 30 bus and IEEE 57 bus test cases excluding and including the insertion of TCSC and Split TCSC through CPF and ACPTDF techniques. The reactance limit value of a TCSC (X_{TCSC}) is taken between -0.8 p.u and 0.2 p.u respectively. In split TCSC, the reactance value can be splitted in to two sections such as X_{TCSC1} and X_{TCSC2}. The values are ranging from -0.8 p.u to -0.3 p.u for X_{TCSC1} and -0.3 p.u to 0.2 p.u for X_{TCSC2} respectively. The optimal location and size of both devices were optimized by Plant Root Foraging Algorithm. In order to apply the proposed methodology in security studies and in congestion management, ATC values are computed in selected transactions with and without FACTS devices. In the studies, the ATC margin is limited by minimum and maximum bus voltage magnitude (in p.u) in the range of 0.95 to 1.05 respectively.

6.1 ATC through CPF

The Available Transfer Capability (ATC) for each of the stipulated source to sink power transfers on IEEE bus test system. Studies are made with two of the FACTs devices like TCSC and Split TCSC to see their effectiveness on enhancing ATC through CPF is validated with IEEE 30 bus and 57 bus test cases.

Table 2
Bilateral Transactions without FACTS for 30 bus system

Cases	Source/sink Bus	ATC in p.u	Line flow violation (Overflow)
Case 1	2/7	1.2239	Line No. 8
Case 2	2/16	1.1754	Line No. 19
Case 3	2/23	1.1992	Line No. 18
Case 4	5/27	1.2169	Line No. 22
Case 5	5/29	1.1825	Line No. 22

Table 3
Bilateral Transactions without FACTS for 57 bus system

Cases	Source/sink Bus	ATC in p.u	Line flow violation (Overflow)
Case 1	3/19	1.2074	Line No. 24
Case 2	3/29	1.1966	Line No. 22
Case 3	6/27	1.1265	Line No. 39
Case 4	6/43	1.1908	Line No. 55
Case 5	12/51	1.1890	Line No. 63

Table 4
Bilateral Transactions with TCSC for 30 bus system

Cases	Source/sink Bus	ATC in p.u	Location	Size
Case 1	2/7	1.4775	Line No. 7	-0.2061
Case 2	2/16	1.3894	Line No. 19	-0.3308
Case 3	2/23	1.4018	Line No. 20	-0.2174
Case 4	5/27	1.3834	Line No. 34	-0.1920
Case 5	5/29	1.2203	Line No. 35	-0.2645

Table 5
Bilateral Transactions with TCSC for 57 bus system

Cases	Source/sink Bus	ATC in p.u	Location	Size X_{TCSC}
Case 1	3/19	1.4017	Line No. 29	-0.3954
Case 2	3/29	1.3998	Line No. 4	-0.6051
Case 3	6/27	1.3016	Line No. 4	-0.5911
Case 4	6/43	1.3384	Line No. 14	-0.6120
Case 5	12/51	1.2993	Line No. 78	-0.4063

Table 6
Bilateral Transactions with Split TCSC for 30 bus system

Cases	Source/Sink Bus	ATC in p.u	Location	Size	
				X_{TCSC1}	X_{TCSC2}
Case 1	2/7	1.5621	Line No. 7	-0.3051	-0.0566
Case 2	2/16	1.4430	Line No. 9	-0.2118	-0.0107
Case 3	2/23	1.4992	Line No. 30	-0.2086	-0.1183
Case 4	5/27	1.4305	Line No. 23	-0.3504	-0.0841
Case 5	5/29	1.3010	Line No. 35	-0.4086	-0.1225

Table 7
Bilateral Transactions with Split TCSC for 57 bus system

Cases	Source/Sink Bus	ATC in p.u	Location	Size	
				X_{TCSC1}	X_{TCSC2}
Case 1	3/19	1.4891	Line No. 12	-0.4006	-0.1558
Case 2	3/29	1.4262	Line No. 4	-0.3922	-0.2852
Case 3	6/27	1.3807	Line No. 4	-0.3116	-0.2120
Case 4	6/43	1.3930	Line No. 14	-0.2869	-0.0953
Case 5	12/51	1.3138	Line No. 61	-0.3937	-0.1077

The entire study of proposed work is divided into two phases. One is the bilateral transactions obtained from seller bus and buyer bus in five cases like 2-7, 2-16, 2-23, 5-27 and 5-29 respectively for IEEE 30 bus system. Another bilateral transaction obtained from seller bus and buyer bus 3-19, 3-29, 6-27, 6-43 and 12-51 respectively for IEEE 57 bus system in five cases also. The ATC values in p.u with respect to the line flow violation without incorporating FACTS devices are given in Table 2 and Table 3 respectively for IEEE 30 and 57 bus test systems.

The ATC values are enhanced after the insertion of TCSC in selected lines. The new enhanced values of ATC in p.u incorporating with TCSC corresponding with transmission line location and size are projected in Table 4 and Table 5 respectively for IEEE 30 and 57 cases.

The enhanced ATC values after the incorporation of Split TCSC in selected lines are superior to the values of ATC incorporated with TCSC. The location of split TCSC is differing from the location of TCSC in case 2, 3 and 4 for IEEE 30 bus test system. Similarly the location of split TCSC is differing from the location of TCSC in case 1 and 5 for IEEE 57 bus test system.

The enhanced values of ATC in p.u incorporating with split TCSC corresponding with transmission line location and splitted TCSC sizes are projected in Table 6 and Table 7 respectively for IEEE 30 and 57 cases.

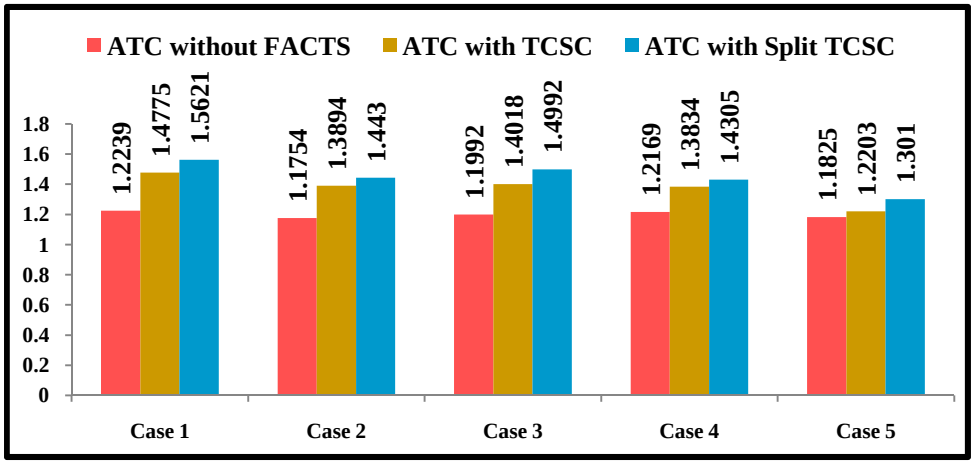

Fig. 5: Comparison of ATC values under all cases for 30 bus system

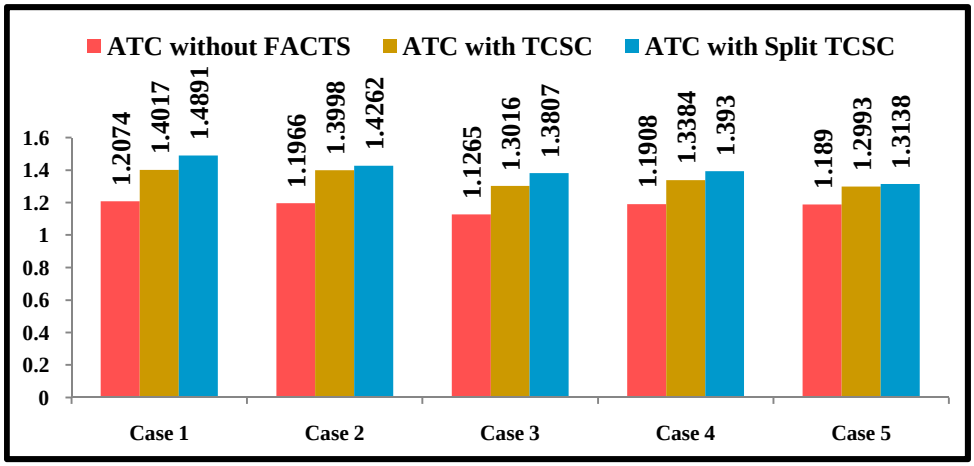

Fig. 6: Comparison of ATC values under all cases for 57 bus system

The comparison of all ATC values without and with TCSC and split TCSC incorporation under all cases for both IEEE 30 and 57 bus test systems are also depicted in figures 5 and 6 respectively. From these comparisons, the ATC enhancement level is superior with incorporation of split TCSC against TCSC.

6.2 ATC through ACPTDF

The Available Transfer Capability (ATC) for each of the stipulated source to sink power transfers on IEEE bus system. Studies are made with two types of the FACTs devices, akin to TCSC and Split TCSC to see their effectiveness on enhancing ATC through ACPTDF is validated with IEEE 30 bus and 57 bus test cases.

The entire study of proposed work is divided into two sections. The first section is the bilateral transaction obtained from seller bus 3 and buyer bus 29 for IEEE 30 bus system and the bilateral transaction obtained from seller bus 5 and buyer bus 29 for IEEE 57 bus system. The second section deals with the Multilateral Transactions (MT) obtained from seller buses 3, 4 and buyer buses 26, 29 respectively for 30 bus system and seller buses 5, 9 and buyer buses 29, 38 respectively for 57 bus system. The global best values of ATC with and without incorporating FACTS devices under the bilateral transaction between seller bus 3 and buyer bus 29 through ACPTDF is given in Table 8 (a). The best location of TCSC and split TCSC with their corresponding values for IEEE 30 bus system is also given in 8(b).

Table 8

Bilateral Transactions between bus 3 and 29 by ACPTDF for 30 bus system

(a) Global best ATC values in p.u

Without FACTS	With TCSC	With Split TCSC
1.1239	1.1408	1.1596

(b) Best location ATC values in p.u 30 bus system

With TCSC		With Split TCSC	
Line No.	ATC values	Line No.	ATC values
7	-0.5502	2	-0.6243
11	-0.0163	11	-0.0224
12	-0.1087	12	-0.0688
15	-0.2680	15	-0.1935
24	-0.6531	24	-0.7110
36	0.0472	36	-0.0067

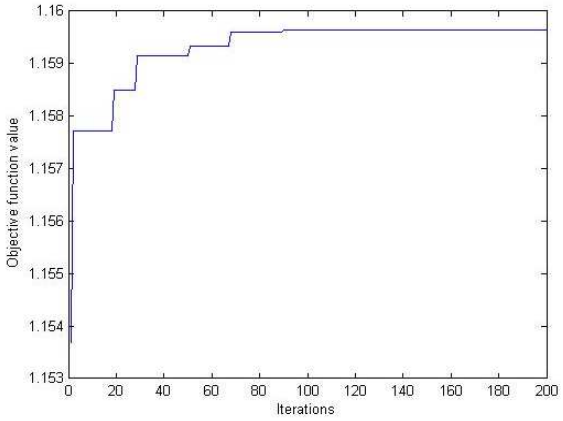

Fig. 7: Convergence characteristics of Split TCSC through BT between bus 3 and 29

Table 9

Bilateral Transactions between bus 5 and 29 by ACPTDF for 57 bus system

(a) Global best ATC values in p.u

Without FACTS	With TCSC	With Split TCSC
1.1239	1.9222	1.9698

(b) Best location ATC values in p.u

With TCSC		With Split TCSC	
Line no.	ATC values	Line no.	ATC values
4	-0.3743	4	-0.2700
12	-0.3107	12	-0.3314
33	-0.0258	24	-0.1992
39	-0.2116	39	-0.4211
57	-0.1171	40	-0.5634
61	-0.3770	79	-0.0698

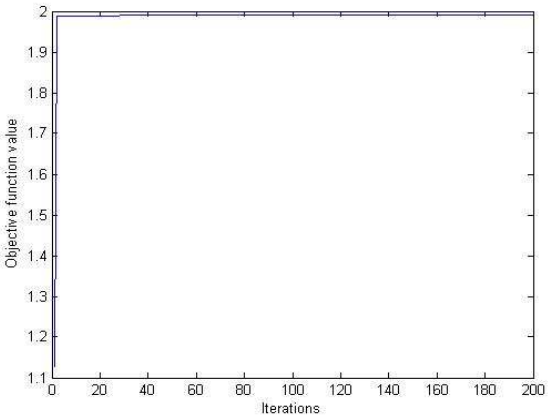

Fig. 8: Convergence characteristics of Split TCSC through BT between bus 5 and 29

The convergence characteristics of split TCSC is given in figure 7. From these results the split TCSC is the best consideration to enhance the ATC through ACPTDF and the difference from without incorporating FACTS devices is 0.0357 p.u and with TCSC insertion is 0.0188 p.u respectively.

Similarly the global best values of ATC with and without incorporating FACTS devices under the bilateral transaction between seller bus 5 and buyer bus 29 through ACPTDF is given in Table 9 (a). The best location of TCSC and split TCSC with their corresponding values for IEEE 57 bus system is also given in 9 (b). The convergence characteristics of split TCSC is given in figure 8. From these results the split TCSC is the best consideration to enhance the ATC through ACPTDF and the difference from without incorporating FACTS devices is 0.07308 p.u and with TCSC insertion is 0.0476 p.u respectively

Table 10

ACPTDF based multilateral transactions (MT) between seller buses 3 and 4 and buyer buses 26 and 29 (30 bus system)

Line No.	From Bus	To Bus	MT Values		
			Without FACTS	With TCSC	With Split TCSC
1	1	2	-0.0072	-0.0152	-0.0177
2	1	3	-0.0109	-0.0074	-0.0121
3	2	4	-0.0528	-0.0185	-0.0193
4	3	4	0.0041	-0.0015	-0.0109
5	2	5	-0.0960	-0.0996	-0.1004
6	2	6	-0.0606	-0.0709	-0.0712
7	4	6	-0.0043	0.0012	-0.0067
8	5	7	0.1084	-0.0029	-0.0085
9	6	7	-0.0509	-0.0674	-0.0677
10	6	8	-0.0014	0.0027	-0.0031
11	6	9	-0.2685	-0.1682	-0.1911
12	6	10	0.0953	-0.0017	-0.0092
13	9	11	-0.3110	-0.2993	-0.3084
14	9	10	-0.1827	-0.1882	-0.1899
15	4	12	-0.0637	-0.0710	-0.7200
16	12	13	-0.4826	-0.4905	-0.4913
17	12	14	-0.3831	-0.3087	-0.3112
18	12	15	-0.2823	-0.2911	-0.2883
19	12	16	0.0016	-0.0045	0.0005
20	14	15	-0.3966	-0.2988	-0.2995
21	16	17	-0.0528	-0.0544	-0.0610
22	15	18	-0.1410	-0.1528	-0.1496
23	18	19	-0.2219	-0.2311	-0.2338
24	19	20	-0.4118	-0.3694	-0.3920
25	10	20	0.0204	-0.0058	-0.0108
26	10	17	-0.2267	-0.2158	-0.2069
27	10	21	-0.0161	0.0020	0.0017
28	10	22	-0.1528	-0.1712	-0.1770
29	21	22	-0.2501	-0.2214	-0.2237
30	15	23	-0.0637	-0.0702	-0.0732
31	22	24	0.1241	0.0963	-0.1066
32	23	24	-0.0826	-0.0991	-0.0998

33	24	25	-0.5911	-0.5983	-0.6041
34	25	26	-0.0398	-0.0401	-0.0442
35	25	27	0.1026	0.1037	0.0928
36	28	27	-0.0365	-0.0425	-0.0441
37	27	29	-0.0584	-0.0541	-0.0559
38	27	30	-0.6348	-0.6337	-0.6351
39	29	30	0.1409	0.1125	0.0963
40	8	28	-0.3205	-0.2821	-0.2868
41	6	28	-0.2917	-0.2980	-0.2991

Table 11

ACPTDF based multilateral transactions (MT) between seller buses 5 and 9 and buyer buses 29 and 38 (57 bus system)

Line No.	From Bus	To Bus	MT Values		
			Without FACTS	With TCSC	With Split TCSC
1	1	2	-0.2088	-0.2110	-0.2096
2	2	3	-0.0362	-0.0396	-0.0399
3	3	4	-0.0067	-0.0102	-0.0109
4	4	5	-0.2616	-0.2647	-0.2682
5	4	6	-0.5133	-0.5142	-0.5110
6	6	7	-0.0952	-0.0971	-0.0988
7	6	8	-0.3030	-0.3042	-0.3056
8	8	9	-0.1478	-0.1497	-0.1490
9	9	10	-0.2685	-0.2671	-0.2699
10	9	11	0.1250	0.0996	-0.1028
11	9	12	-0.0665	-0.0670	-0.0683
12	9	13	-0.0977	-0.0961	-0.0994
13	13	14	-0.4158	-0.4083	-0.4112
14	13	15	-0.1401	-0.1416	-0.1504
15	1	15	0.2377	0.2120	0.2084
16	1	16	-0.1598	-0.1586	-0.1606
17	1	17	-0.0036	-0.0048	-0.0057
18	3	15	-0.0054	-0.0073	-0.0080
19	4	18	-0.0856	-0.0962	-0.0974
20	4	18	-0.0856	-0.0962	-0.0974
21	5	6	-0.0457	-0.0459	-0.0471
22	7	8	-0.3652	-0.3661	-0.3624
23	10	12	-0.2541	-0.2528	-0.2555
24	11	13	0.3118	0.2996	0.2934
25	12	13	-0.0051	-0.0073	-0.0091
26	12	16	-0.3574	-0.3580	-0.3591
27	12	17	-0.0658	-0.0639	-0.0671
28	14	15	-0.2160	-0.2094	-0.2097
29	18	19	-0.0453	-0.0483	-0.0473
30	19	20	-0.6911	-0.6924	-0.6880
31	21	20	-0.4421	-0.4428	-0.4447
32	21	22	-0.0036	-0.0080	-0.0093
33	22	23	0.1203	0.1179	0.1165
34	23	24	0.0224	0.0215	0.0207
35	24	25	-0.0325	-0.0357	-0.0361
36	24	25	-0.0325	-0.0357	-0.0361
37	24	26	-0.3941	-0.3946	-0.3948
38	26	27	-0.0325	-0.0329	-0.0341
39	27	28	0.0037	-0.0004	-0.0056
40	28	29	-0.0142	-0.0159	-0.0187
41	7	29	-0.4954	-0.4920	-0.4882
42	25	30	-0.3620	-0.3661	-0.3637
43	30	31	-0.0258	-0.0277	-0.0281
44	31	32	-0.0637	-0.0591	-0.0593
45	32	33	-0.0601	-0.0610	-0.0658
46	34	32	-0.1325	-0.1328	-0.1337
47	34	35	-0.2007	-0.2014	-0.2113
48	35	36	0.1201	0.1194	0.1191
49	36	37	-0.3014	-0.3017	-0.3014
50	37	38	-0.0570	-0.0579	-0.0584
51	37	39	-0.0037	-0.0062	0.0078
52	36	40	-0.2013	-0.2019	-0.2027
53	22	38	-0.0811	-0.0827	-0.0830
54	11	41	0.2037	0.2010	0.2004
55	41	42	-0.2057	-0.2059	-0.2057
56	41	43	-0.3111	-0.3128	-0.3122
57	38	44	-0.0853	-0.0893	-0.0907
58	15	45	-0.0147	-0.0151	-0.0159
59	14	46	-0.3254	-0.3258	-0.3119
60	46	47	-0.1896	-0.1882	-0.1918
61	47	48	-0.0392	-0.0401	-0.0426
62	48	49	0.1772	0.1689	0.1683
63	49	50	0.0322	0.0357	0.0348
64	50	51	-0.3381	-0.3391	-0.3393
65	10	51	-0.4837	-0.4902	-0.4897
66	13	49	-0.2931	-0.2937	-0.2939
67	29	52	-0.0074	-0.0097	-0.0106
68	52	53	-0.0993	-0.1006	-0.1053
69	53	54	-0.5227	-0.5184	-0.5191
70	54	55	-0.1496	-0.1419	-0.1452
71	11	43	0.2041	0.2088	0.2087
72	44	45	0.0821	0.0826	0.0811
73	40	56	-0.1256	-0.1285	-0.1288
74	56	41	-0.4112	-0.4167	-0.4159
75	56	42	-0.0582	-0.0580	-0.0597
76	39	57	-0.3105	-0.3096	-0.3098
77	57	56	-0.6362	-0.6284	-0.6281
78	38	49	-0.2508	-0.2543	-0.2553
79	38	48	-0.1987	-0.1994	-0.1997
80	9	55	-0.1047	-0.1053	-0.1067

The Multilateral Transactions is obtained from seller buses 3, 4 and buyer buses 26, 29 respectively for 30 bus system and seller buses 5, 9 and buyer buses 29, 38 respectively for 57 bus system. The line wise ATC values with and without incorporating FACTS devices through ACPTDF are given in Table 10 and Table 11 respectively. Obviously it is proved that the enhanced ATC values are improved through the incorporation of split TCSC on both test cases.

7. Conclusion

The enhancement of ATC incorporating TCSC and split TCSC through CPF and ACPTDF is studied with IEEE 30 and IEEE 57 bus test systems

during absence and presence of FACTS devices. Two bilateral transactions under five cases are observed in CPF and two bilateral transactions with one multi lateral transaction are observed in ACPTDF. The size and location of FACTS devices were optimized by Plant Root Foraging Algorithm. It is shown that while TCSC and split TCSC can get better ATC in thermal dominant case. The results are obviously showed that split TCSC is more effective in improving ATC than TCSC under normal situation.

References:

[1] "*IEEE Reliability Test System*", IEEE Transactions on Power Apparatus and Systems, Vol. PAS-98, No.6, pp: 121-129, 1979.

[2] Transmission Transfer Capability Task Force, "*Available Transfer Capability Definitions and Determination*", North American Electric Reliability Council, New Jersey, 1996.

[3] Ajarapu V, Christie C. "*The continuation power flow: A Practical Tool for Tracing Power System Steady State Stationary behaviour due to the Load and Generation Variations*". IEEE Transactions on Power Systems, Vol.7, No.1, pp: 416-423, 1992.

[4] Dai Y, McCalley J.D and Vittal V. "*Simplification, Expansion and Enhancement of Direct Interior Point Algorithm for Power System Maximum Loadability*", Proceedings of 21st International Conference on Power Industrial Computer Applications, pp: 170-179, 1999.

[5] Christie R.D, Wollenberg B.F and Wangstien I. "*Transmission management in the deregulated environment*". Proceedings of IEEE, Vol.88, No: 2, pp: 170–95.

[6] Kumar J and Kumar A, "*Multi-Transactions ATC Determination using PTDFs based Approach in Deregulated Markets*", Proceedings of Annual Power India conference (INDICON); pp. 1–6. 2011.

[7] Ejebe G.C, Tong J, Waight G.G, Frame J.G, Wang X and Tinney W.F. "*Available Transfer Capability Calculations*". IEEE Transactions on Power System, Vol.13, No.4, pp: 1521-1527, 1998.

[8] Gravener M.H and Nwankpa C. "*Available Transfer Capability and First Order Sensitivity*". IEEE Transactions on Power System, Vol.14, No.2, pp: 512-518, 1999.

[9] Ejebe G.C, Waight J.G, Santos-Nieto M and Tinney W.F. "*Fast Calculation of Linear Available Transfer Capability*". IEEE Transactions on Power System, Vol.15, No.3, pp: 1112-1116, 2000.

[10] Grijalva S, Sauer PW, Weber JD. Enhancement of linear ATC calculations by the incorporation of reactive power flows. IEEE Transactions on Power System, Vol.18, No:2, pp:619–624, 2003.

[11] Kumar A, Srivastava S.C and Singh S.N. "*Available Transfer Capability (ATC) Determination in Competitive Electricity Market using AC Distribution Factors*". Electric Power Components and Systems, Vol.32, No.9, pp: 927-939, 2010.

[12] Greene S, Dobson I, Alvarado FL. "*Sensitivity of Transfer Capability Margin with a Fast Formula*". IEEE Transactions on Power System, Vol.17, No: 1, pp: 34-40, 2002.

[13] Li C.Y and Liu C.W. "*A New Algorithm for Available Transfer Capability Calculation*", Electric Power and Energy System, Vol.24, No.1, pp: 159-166, 2002.

[14] Kumar J and Kumar A. "*ACPTDF for Multi-Transactions and ATC Determination in Deregulated Markets*". International Journal of Electrical and Computer Engineering Vol.1, No.1, pp: 71-84, 2011.

[15] Xiao Y, Song Y.H and Sun Y.Z. "Available Transfer Capability Enhancement using FACTS Devices". Proceedings of IEEE /PWS Summer Meeting, Seattle, pp: 508-515, 2000.

[16] Feng W and Shrestha G.B. "*Allocation of TCSC Devices to Optimize Total Transmission Capacity in a Competitive Power Market*", IEEE Transactions on Power Systems, Vol.2, No.1, pp: 587-593, 2001.

[17] Gerbex S, Cherkaoui R and Germond A.J. "*Optimal Location of Multi-Type FACTS Devices in a Power System by Means of Genetic Algorithms*". IEEE Transactions on Power Systems, Vol.6, No.4, pp: 537-544, 2001.

[18] Rashidinejad M, Farahmand H, Fotuhi-Firuzabad M and Gharaveisi A.A. "*ATC Enhancement Using TCSC via Artificial Intelligent Techniques*". Electric Power System Research, Vol.78, No.1, pp: 11-20, 2008.

[19] Jebaraj L, Muralikrishnan N, Christober Asir Rajan C, "*DE Algorithm based Comparison between Two Different Combinations of FACTS Devices under Single Line Outage Contingency Condition*", IEEE International Conference on Intelligent Systems and Control, pp: 158-165, 2013.

[20] Meikandasivam S, Nemab R.K and Jain S.K, "*Fine Power Flow Control by Split TCSC*", Electrical Power Energy Systems, Vol.45, No.3, pp: 519-529, 2012.

[21] Lianbo M, Kunyuan H, Yunlong Z, Hanning C and Maowei H, "*A Novel Plant Root Foraging Algorithm for Image Segmentation Problems*", Mathematical Problems in Engineering, Volume 2014, pp: 1-16, 2014.

[22] McNickle G, Clair C. and Cahill J.F "*Focusing the metaphor: plant root foraging behaviour*," Trends in Ecology and Evolution, vol. 24, No. 8, pp. 419–426, 2009.